Precision benchmark calculations for four particles at unitarity

Shahin Bour,[1] Xin Li,[2] Dean Lee,[2] Ulf-G. Meißner,[1,3] and Lubos Mitas[2]

[1]*Helmholtz-Institut für Strahlen- und Kernphysik (Theorie) and Bethe Center for Theoretical Physics, Universität Bonn, D-53115 Bonn, Germany*

[2]*Department of Physics, North Carolina State University, Raleigh, North Carolina 27695, USA*

[3]*Institut für Kernphysik (IKP-3), Institute for Advanced Simulation (IAS-4), and Jülich Center for Hadron Physics, Forschungszentrum Jülich, D-52425 Jülich, Germany*

The unitarity limit describes interacting particles where the range of the interaction is zero and the scattering length is infinite. We present precision benchmark calculations for two-component fermions at unitarity using three different *ab initio* methods: Hamiltonian lattice formalism using iterated eigenvector methods, Euclidean lattice formalism with auxiliary-field projection Monte Carlo methods, and continuum diffusion Monte Carlo methods with fixed and released nodes. We have calculated the ground-state energy of the unpolarized four-particle system in a periodic cube as a dimensionless fraction of the ground-state energy for the noninteracting system. We obtain values of 0.211(2) and 0.210(2) using two different Hamiltonian lattice representations, 0.206(9) using Euclidean lattice formalism, and an upper bound of 0.212(2) from fixed-node diffusion Monte Carlo methods. Released-node calculations starting from the fixed-node result yield a decrease of less than 0.002 over a propagation of $0.4E_F^{-1}$ in Euclidean time, where E_F is the Fermi energy. We find good agreement among all three *ab initio* methods.

PACS number(s): 03.75.Ss, 02.70.Ss, 24.10.Cn, 21.65.Cd

I. INTRODUCTION

The unitarity limit describes interacting particles where the range of the interaction is zero and the *S*-wave scattering length is infinite. In this paper we consider the unitarity limit of two-component fermions. Throughout our discussion we refer to the two degenerate components as up and down spins, though the correspondence with actual spin is not necessary. At sufficiently low temperatures the spin-unpolarized system is an *S*-wave superfluid with properties in between a Bardeen-Cooper-Schrieffer (BCS) fermionic superfluid at weak coupling and a Bose-Einstein condensate of dimers at strong coupling [1–3]. In nuclear physics the phenomenology of the unitarity limit approximately describes cold dilute neutron matter. The scattering length for elastic neutron-neutron collisions is about −18 fm, while the range of the interaction is roughly the Compton wavelength of the pion, 1.4 fm. The unitarity limit is approximately realized when the interparticle spacing is about 5 fm. While these conditions cannot be produced experimentally, neutrons at around this density can be found in the inner crust of neutron stars.

Experimental probes of the unitarity limit are now well established using trapped ultracold Fermi gases of alkali atoms. The characteristic length scale for the interatomic potential is the van der Waals length $\ell_{\rm vdW}$. In the dilute limit the spacing between atoms can be made much larger than $\ell_{\rm vdW}$, and the interatomic potential is well approximated by a zero-range interaction. The *S*-wave scattering length can be tuned using a magnetic Feshbach resonance [4–8]. This technique involves setting the energy level for a molecular bound state in a "closed" hyperfine channel to cross the scattering threshold for the "open" channel. The total magnetic moments for the two channels are different, and so the crossing can be produced using an applied magnetic field.

The ground state for two-component fermions in the unitarity limit has no physical length scales other than the average distance between particles. The scaling properties in the unitarity limit are the same as those of a noninteracting Fermi gas. For $N_\uparrow$ up spins and $N_\downarrow$ down spins in a given volume we write the energy of the unitarity-limit ground state as $E_{N_\uparrow,N_\downarrow}^0$. For the same volume we call the energy of the free, noninteracting ground state $E_{N_\uparrow,N_\downarrow}^{0,\rm free}$. In the following we write the dimensionless ratio of the two energies as $\xi_{N_\uparrow,N_\downarrow}$,

$$\xi_{N_\uparrow,N_\downarrow} = E_{N_\uparrow,N_\downarrow}^0 \big/ E_{N_\uparrow,N_\downarrow}^{0,\rm free}. \tag{1}$$

The parameter ξ is defined as the thermodynamic limit for the spin-unpolarized system,

$$\xi = \lim_{N\to\infty} \xi_{N,N}. \tag{2}$$

II. RESULTS FOR ξ AND THE NEED FOR PRECISION BENCHMARKS

Several experiments have measured ξ using the expansion rate of ^{6}Li and ^{40}K released from a harmonic trap as well as sound propagation. Some recent measured values for ξ are 0.32^{+13}_{-10} [9], 0.36(15) [10], 0.51(4) [11], 0.46(5) [12], 0.46^{+05}_{-12} [13], 0.435(15) [14], 0.41(15) [15], 0.41(2) [16], and 0.39(2) [16]. Another preliminary measurement finds a value 0.36(1) [17].

There are numerous analytical calculations of ξ using a variety of techniques, such as saddle-point and variational approximations [18,19], Padé approximations and truncated series methods [20–22], mean-field theory with pairing [23,24], density-functional theory extrapolated from small systems [25], renormalization-group flow [26], dimensional expansions [27–33], large-N expansions [34], and other methods [35]. The values for ξ range from 0.2 to 0.6, with most predictions in the range from 0.3 to 0.4.

There are also many numerical calculations for ξ. The earliest fixed-node diffusion Monte Carlo simulations for N spin-up and N spin-down fermions in a periodic cube found $\xi_{N,N}$ to be 0.44(1) for $5 \leqslant N \leqslant 21$ [36] and 0.42(1) for larger N [37,38]. A restricted path-integral Monte Carlo calculation found similar results [39], and a sign-restricted mean-field lattice calculation yields 0.449(9) [40]. Another fixed-node diffusion Monte Carlo calculation sets an upper bound for $\xi_{N,N}$ at 0.4244(1) for $N = 33$ and 0.4339(1) for $N = 64$ [41]. A more recent fixed-node calculation sets an upper bound for $\xi_{N,N}$ at 0.383(1) for N between 2 and 65 [42]. This study includes an extrapolation to the zero-range limit and an analysis of shell effects using density-functional theory. We note that methods such as the fixed-node diffusion Monte Carlo method provide only an upper bound for the ground-state energy. An unbiased estimate for the ground-state energy requires releasing the nodal constraint over a propagation time comparable to the diffusion time for neighboring particles to cross paths.

There have also been a number of lattice simulations of two-component fermions in the unitarity limit. Several lattice simulations for the average energy at nonzero temperature have been extrapolated to the zero-temperature limit. The extrapolated zero-temperature results from [43,44] established a bound, $0.07 \leqslant \xi \leqslant 0.42$. The results of Ref. [45] as well as Ref. [46,47] produce a value for ξ in the 0.3 to 0.5 range. More recent lattice calculations extrapolated to zero temperature yield values of $\xi = 0.292(24)$ [48,49] and $\xi = 0.37(5)$ [50].

In Ref. [51] the ground-state energy was calculated on the lattice using auxiliary-field Monte Carlo methods and Euclidean time projection starting from an initial state. The values of $\xi_{N,N}$ for $N = 3,5,7,9,11$ were calculated at lattice volumes $4^3, 5^3, 6^3$ in units of lattice spacing. From these small volumes it was estimated that $\xi = 0.25(3)$. In Ref. [52] this lattice calculation was improved using bounded continuous auxiliary fields. This calculation included an extrapolation to the continuum limit for $\xi_{5,5}$ and $\xi_{7,7}$ using lattice volumes $4^3, 5^3, 6^3, 7^3, 8^3$. The results obtained were $\xi_{5,5} = 0.292(12)$ and $\xi_{7,7} = 0.329(5)$. Another technique called the symmetric heavy-light ansatz found similar values for $\xi_{N,N}$. While this approach is not an *ab initio* method, the agreement with the values for $\xi_{5,5}$ and $\xi_{7,7}$ in Ref. [52] were within an error of 0.015. This method gives an estimate of $\xi = 0.31(1)$ in the continuum and thermodynamic limits [53]. Another extrapolation of the same data using density-functional theory to include shell effects yields a value of $\xi = 0.322(2)$ [42]. Some newer but preliminary lattice calculations using different projection and sampling methods produce a value of $\xi_{N,N} = 0.412(4)$ for N in the range from 8 to 19 [54,55].

The physics of the unitarity limit is universal and can be observed in many different systems and calculated using many different methods. However, the spread in experimental, analytical, and numerical evaluations for $\xi_{N,N}$ and ξ highlights the need for precision benchmarks and a more careful understanding of residual errors. Benchmarks at unitarity have been a subject of much discussion at several recent workshops and programs at the Institute for Nuclear Theory in Seattle. In this paper we discuss benchmarks for four unpolarized particles in a periodic cube. We focus on first-principles numerical calculations for $\xi_{2,2}$ where all stochastic,

extrapolation, and systematic errors can be reliably estimated. The three calculations we compare are the Hamiltonian lattice formalism using iterated eigenvector methods, Euclidean lattice formalism with auxiliary-field projection Monte Carlo methods, and continuum diffusion Monte Carlo methods with fixed and released nodes.

III. NOTATION AND DEFINITIONS

Let $E_{N_\uparrow, N_\downarrow}^{0,\text{free}}$ be the ground-state energy for $N_\uparrow$ up-spin and $N_\downarrow$ down-spin free fermions with equal masses in a periodic cube. We write $E_{N_\uparrow, N_\downarrow}^0$ for the ground-state energy at unitarity for the same particle numbers, $N_\uparrow$ and $N_\downarrow$, and the same periodic cube. In the introduction we defined the energy ratio,

$$\xi_{N_\uparrow, N_\downarrow} = E_{N_\uparrow, N_\downarrow}^0 \big/ E_{N_\uparrow, N_\downarrow}^{0,\text{free}}. \tag{3}$$

We should point out that there are actually two different conventions for $\xi_{N_\uparrow, N_\downarrow}$ used in the literature. We refer to Eq. (3) as the few-body definition for the energy ratio $\xi_{N_\uparrow, N_\downarrow}$. This is the definition we use for all calculations presented here.

The alternative definition for the energy ratio $\xi_{N_\uparrow, N_\downarrow}$ is what we call the thermodynamical definition. This involves replacing $E_{N_\uparrow, N_\downarrow}^{0,\text{free}}$ by the formula one gets in the thermodynamic limit. We define the Fermi momenta and energies in terms of the particle density,

$$k_{F,\uparrow} = \left(6\pi^2 \frac{N_\uparrow}{L^3}\right)^{1/3}, \quad k_{F,\downarrow} = \left(6\pi^2 \frac{N_\downarrow}{L^3}\right)^{1/3}, \tag{4}$$

$$E_{F,\uparrow} = \frac{k_{F,\uparrow}^2}{2m}, \quad E_{F,\downarrow} = \frac{k_{F,\downarrow}^2}{2m}. \tag{5}$$

In the thermodynamic limit the ground-state energy of the noninteracting system is

$$\tfrac{3}{5} N_\uparrow E_{F,\uparrow} + \tfrac{3}{5} N_\downarrow E_{F,\downarrow}. \tag{6}$$

We use this to define the thermodynamical definition of the energy ratio,

$$\xi_{N_\uparrow, N_\downarrow}^{\text{thermo}} = \frac{E_{N_\uparrow, N_\downarrow}^0}{\tfrac{3}{5} N_\uparrow E_{F,\uparrow} + \tfrac{3}{5} N_\downarrow E_{F,\downarrow}}. \tag{7}$$

For finite $N_\uparrow$ and $N_\downarrow$ the few-body ratio $\xi_{N_\uparrow, N_\downarrow}$ and thermodynamical ratio $\xi_{N_\uparrow, N_\downarrow}^{\text{thermo}}$ differ due to shell effects in the noninteracting system. There are several calculations in the literature using each of these two alternative definitions. In Table I we have tabulated the conversion between the two definitions for several values of particle number with $N_\uparrow = N_\downarrow$.

IV. HAMILTONIAN LATTICE WITH SPARSE-MATRIX EIGENVECTOR ITERATION

A. Formalism and notation

Let $\vec{n}$ denote spatial lattice points on a three-dimensional $L \times L \times L$ periodic cube. We use lattice units where physical quantities are multiplied by powers of the spatial lattice spacing to make the combination dimensionless. The two-component fermions are labeled as spin up and spin down, and

TABLE I. Conversion factor between the two ground-state ratios $\xi_{N_\uparrow,N_\downarrow}$ and $\xi_{N_\uparrow,N_\downarrow}^{\text{thermo}}$ for various values of $N_\uparrow = N_\downarrow$.

$N_\uparrow = N_\downarrow$	$\xi_{N_\uparrow,N_\downarrow}/\xi_{N_\uparrow,N_\downarrow}^{\text{thermo}}$	$N_\uparrow = N_\downarrow$	$\xi_{N_\uparrow,N_\downarrow}/\xi_{N_\uparrow,N_\downarrow}^{\text{thermo}}$
2	0.7331	8	0.9236
3	0.7204	9	0.8991
4	0.7758	10	0.8931
5	0.8439	16	0.9774
6	0.9149	24	1.0246
7	0.9858	32	1.0064

the lattice annihilation operators are written as $a_\uparrow(\vec{n})$ and $a_\downarrow(\vec{n})$. We start with the free nonrelativistic lattice Hamiltonian,

$$H_{\text{free}} = \frac{3}{m} \sum_{\vec{n},i=\uparrow,\downarrow} a_i^\dagger(\vec{n})a_i(\vec{n}) - \frac{1}{2m} \sum_{l=1,2,3} \sum_{\vec{n},i=\uparrow,\downarrow} [a_i^\dagger(\vec{n})a_i(\vec{n}+\hat{l})$$
$$+ a_i^\dagger(\vec{n})a_i(\vec{n}-\hat{l})]. \tag{8}$$

We define the spin-density operators

$$\rho_\uparrow(\vec{n}) = a_\uparrow^\dagger(\vec{n})a_\uparrow(\vec{n}), \tag{9}$$

$$\rho_\downarrow(\vec{n}) = a_\downarrow^\dagger(\vec{n})a_\downarrow(\vec{n}). \tag{10}$$

We consider two different lattice Hamiltonians, each of which yield the unitarity limit in the low-energy limit. The first Hamiltonian H_1 has a single-site contact interaction,

$$H_1 = H_{\text{free}} + C_1 \sum_{\vec{n}} \rho_\uparrow(\vec{n})\rho_\downarrow(\vec{n}). \tag{11}$$

The coefficient of C_1 is tuned to set the S-wave scattering length a_0 to infinity. The second Hamiltonian H_2 has a contact interaction as well as nearest-neighbor interaction terms,

$$H_2 = H_{\text{free}} + C_2 \sum_{\vec{n}} \rho_\uparrow(\vec{n})\rho_\downarrow(\vec{n})$$
$$+ C_2' \sum_{l=1,2,3} \sum_{\vec{n}} [\rho_\uparrow(\vec{n})\rho_\downarrow(\vec{n}+\hat{l}) + \rho_\uparrow(\vec{n}+\hat{l})\rho_\downarrow(\vec{n})]. \tag{12}$$

The coefficients C_2 and C_2' are tuned so that a_0 goes to infinity while the S-wave effective range parameter r_0 vanishes.

We use Lüscher's formula [56–59] to determine the unknown interaction coefficients C_1, C_2, and C_2'. Lüscher's formula relates the two-particle energy levels in a length L periodic cube to the S-wave phase shift,

$$p \cot \delta_0(p) = \frac{1}{\pi L} S(\eta), \qquad \eta = \left(\frac{Lp}{2\pi}\right)^2, \tag{13}$$

where $S(\eta)$ is the three-dimensional ζ function,

$$S(\eta) = \lim_{\Lambda \to \infty} \left[\sum_{\vec{n}} \frac{\theta(\Lambda^2 - \vec{n}^2)}{\vec{n}^2 - \eta} - 4\pi\Lambda \right]. \tag{14}$$

In terms of η, the energy of the two-particle scattering state is

$$E_{\text{pole}} = \frac{p^2}{m} = \frac{\eta}{m}\left(\frac{2\pi}{L}\right)^2. \tag{15}$$

The S-wave effective range expansion gives

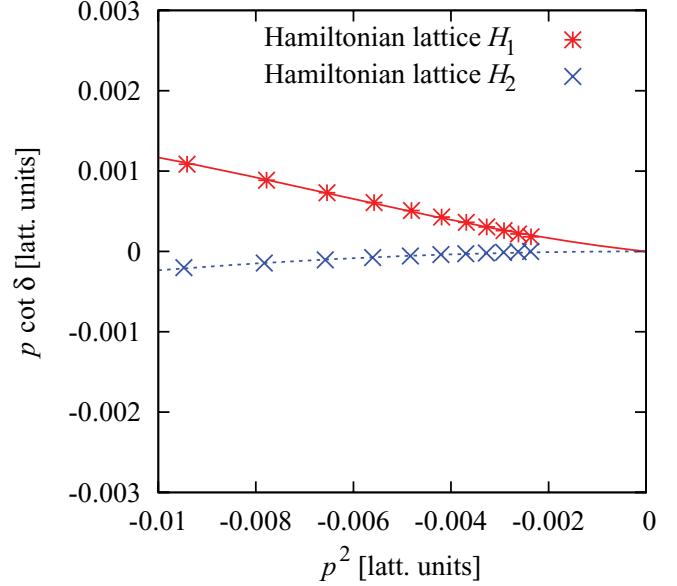$$p \cot \delta_0(p) = -\frac{1}{a_0} + \frac{1}{2}r_0 p^2 + O(p^4). \tag{16}$$

FIG. 1. (Color online) Plot of $p \cot \delta_0(p)$ versus p^2 for the lattice Hamiltonians H_1 and H_2.

Setting a_0 to infinity requires $p \cot \delta_0(p)$ to vanish at threshold. Setting both a_0 to infinity and r_0 to zero requires that $p \cot \delta_0(p)$ is $O(p^4)$ near threshold. The plots for $p \cot \delta_0(p)$ versus p^2 are shown in Fig. 1. The values we find for the interaction coefficients are

$$mC_1 = -3.9570, \tag{17}$$

$$mC_2 = -3.7235, \qquad mC_2' = -0.3008. \tag{18}$$

B. Results for the four-particle benchmark

Using the Lanczos algorithm for sparse-matrix eigenvector iteration [60], we have computed the ground-state energy for two spin-up and two spin-down particles in a periodic cube of length L. For both lattice Hamiltonians, H_1 and H_2, we have computed $\xi_{2,2}$ as defined in Eq. (3) for values of $L = 4,5,6,7,8$. The results are shown in Fig. 2.

We have fitted the data using polynomials in $1/L$ up to third order and extrapolate to the infinite L limit with an estimated extrapolation error of ± 0.002. We note that this extrapolation should remove all measurable lattice discretization effects. For H_1 we find

$$\xi_{2,2} = 0.211(2), \tag{19}$$

and for H_2 we get

$$\xi_{2,2} = 0.210(2). \tag{20}$$

The agreement between these two independent calculations is consistent with our estimate of the systematic errors.

The third-degree polynomial extrapolation is made possible by the high-precision data obtained for each L using the Lanczos eigenvector iteration. For the Monte Carlo data appearing later in our discussion we use only linear extrapolations in $1/L$. For the H_2 data we note the small slope in $1/L$ near $1/L = 0$. This is expected due to the effective range r_0 being set to zero for H_2. The small amount of linear dependence in $1/L$ that remains is likely due to other lattice artifacts, such as the breaking of Galilean invariance [61].
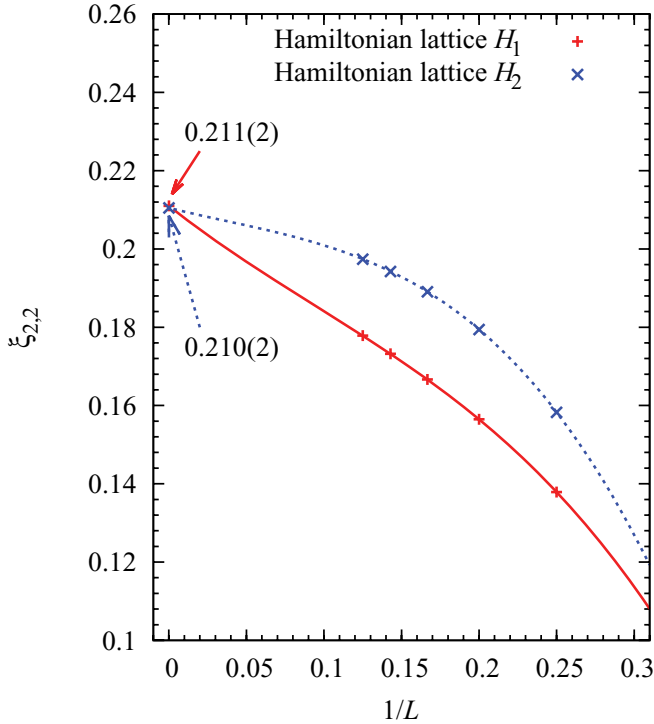
FIG. 2. (Color online) Ground-state energy ratio $\xi_{2,2}$ for lattice Hamiltonians H_1 and H_2. We show results for values of $L = 4,5,6,7,8$ and extrapolate to the infinite volume limit.

V. EUCLIDEAN LATTICE WITH AUXILIARY-FIELD PROJECTION MONTE CARLO METHODS

A. Formalism and notation

For the Euclidean lattice calculation we use the normal-ordered transfer-matrix formalism used in Ref. [51,52,62,63]. Normal ordering refers to the rearrangement of operators with annihilation operators on the right and creation operators on the left. This prescription is useful in that it provides an exact relation between Grassmann path integration and the operator formalism [64,65]. The details of the application of this correspondence can be found in Refs. [52,62,63]. As before we use lattice units that correspond to multiplying physical quantities by the corresponding power of the spatial lattice spacing to make the combination dimensionless. We write $\alpha_t = a_t/a$ for the dimensionless ratio of the temporal lattice spacing to spatial lattice spacing. For fermion mass m, we take the ratio of lattice spacings so that $m^{-1}\alpha_t = 0.1109$.

We start with the normal-ordered transfer matrix operator,

$$M = \, : \exp\left[-H_{\text{free}}\alpha_t - C\alpha_t \sum_{\vec{n}} \rho_\uparrow(\vec{n})\rho_\downarrow(\vec{n}) \right] : . \quad (21)$$

The free lattice Hamiltonian H_{free} was defined in Eq. (8), and the spin densities were defined Eqs. (9) and (10). Just as in the Hamiltonian lattice calculation we use Lüscher's formula to determine the unknown coefficient C. Setting the S-wave scattering length to infinity, we find

$$mC = -3.4938. \quad (22)$$

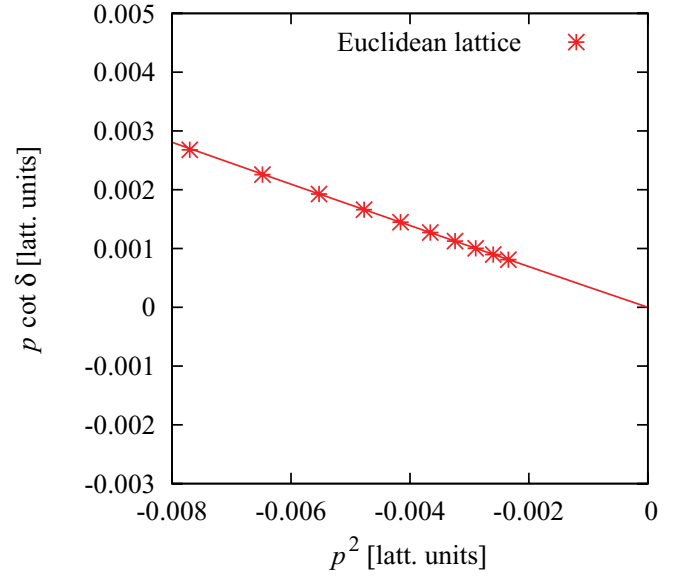In Fig. 3 we plot $p \cot \delta_0(p)$ versus p^2 at unitarity.

FIG. 3. (Color online) Plot of $p \cot \delta_0(p)$ versus p^2 for the Euclidean time lattice formalism.

For the Monte Carlo simulations we use the bounded continuous auxiliary-field transformation introduced in Ref. [52]. This transformation was shown in Ref. [52] to have performance advantages over other continuous and discrete auxiliary-field transformations. We can write the transfer matrix as

$$M = \prod_{\vec{n}} \left[\frac{1}{2\pi} \int_{-\pi}^{+\pi} ds(\vec{n},n_t) \right] M(s,n_t), \quad (23)$$

where

$$M(s,n_t) = \, : \exp\left\{ -H_{\text{free}}\alpha_t + \sum_{\vec{n}} \sqrt{-2C\alpha_t} \sin[s(\vec{n},n_t)] \right.$$
$$\left. \times [\rho_\uparrow(\vec{n}) + \rho_\downarrow(\vec{n})] \right\} : . \quad (24)$$

Let $|\Psi_{2,2}^{\text{init}}\rangle$ be a Slater determinant of single-particle normal modes composed of two spin-up fermions and two spin-down fermions,

$$\left| \Psi_{2,2}^{\text{init}} \right\rangle = |\psi_1\rangle \times |\psi_2\rangle \times |\psi_3\rangle \times |\psi_4\rangle. \quad (25)$$

For the calculations presented here we choose

$$|\psi_1\rangle = \sqrt{\frac{1}{L^3}} \sum_{\vec{n}} a_\uparrow^\dagger(\vec{n})|0\rangle,$$

$$|\psi_2\rangle = \sqrt{\frac{2}{L^3}} \sum_{\vec{n}} \cos(2\pi n_3/L) a_\uparrow^\dagger(\vec{n})|0\rangle, \quad (26)$$

$$|\psi_3\rangle = \sqrt{\frac{1}{L^3}} \sum_{\vec{n}} a_\downarrow^\dagger(\vec{n})|0\rangle,$$

$$|\psi_4\rangle = \sqrt{\frac{2}{L^3}} \sum_{\vec{n}} \cos(2\pi n_3/L) a_\downarrow^\dagger(\vec{n})|0\rangle. \quad (27)$$

$|\psi_1\rangle$ and $|\psi_3\rangle$ are constant valued throughout the periodic box, while $|\psi_2\rangle$ and $|\psi_4\rangle$ are standing waves with wavelength L

along the z axis. We construct the Euclidean time projection amplitude

$$Z_{2,2}(t) \equiv \prod_{\vec{n},n_t} \left[\frac{1}{2\pi} \int_{-\pi}^{+\pi} ds(\vec{n},n_t) \right]$$
$$\times \langle \Psi_{2,2}^{\text{init}} | M(s,L_t-1) \cdots M(s,0) | \Psi_{2,2}^{\text{init}} \rangle, \quad (28)$$

where the Euclidean projection time t equals L_t times the temporal lattice spacing.

Each $M(s,n_t)$ consists of only single-particle operators interacting with the background auxiliary field. Therefore, we find

$$\langle \Psi_{2,2}^{\text{init}} | M(s,L_t-1) \cdots M(s,0) | \Psi_{2,2}^{\text{init}} \rangle = [\det \mathbf{M}(s,t)]^2, \quad (29)$$

where

$$[\mathbf{M}(s,t)]_{k'k} = \langle \psi_{k'} | M(s,L_t-1) \cdots M(s,0) | \psi_k \rangle \quad (30)$$

for matrix indices $k,k' = 1,2,3,4$. We define a t-dependent energy expectation value,

$$E_{2,2}(t) = \frac{1}{\alpha_t} \ln \frac{Z_{2,2}(t-\alpha_t)}{Z_{2,2}(t)}. \quad (31)$$

We can also express the t-dependent expectation value as a fraction of the noninteracting ground-state energy,

$$\xi_{2,2}(t) = E_{2,2}(t) \big/ E_{2,2}^{0,\text{free}}. \quad (32)$$

The ground-state energy $E_{N,N}^0$ is given by the limit

$$E_{2,2}^0 = \lim_{t \to \infty} E_{2,2}(t), \quad (33)$$

and the desired few-body energy ratio can be computed as the limit

$$\xi_{2,2} = \lim_{t \to \infty} \xi_{2,2}(t). \quad (34)$$

B. Results for the four-particle benchmark

For the calculation of $\xi_{2,2}(t)$ we use the lattice dimensions $L^3 \times L_t$ shown in Table II. The simulations are run with 2048 processors each independently generating 3000 hybrid Monte Carlo trajectories [66–68]. To extract $\xi_{2,2}$ we perform a least-squares fit of $\xi_{2,2}(t)$ to the asymptotic form,

$$\xi_{2,2}(t) = \xi_{2,2} + b e^{-\delta E t}. \quad (35)$$

This exponential form takes into account the contribution from higher-energy states and is the same method used

TABLE II. Lattice dimensions $L^3 \times L_t$ used in calculations for $\xi_{2,2}(t)$.

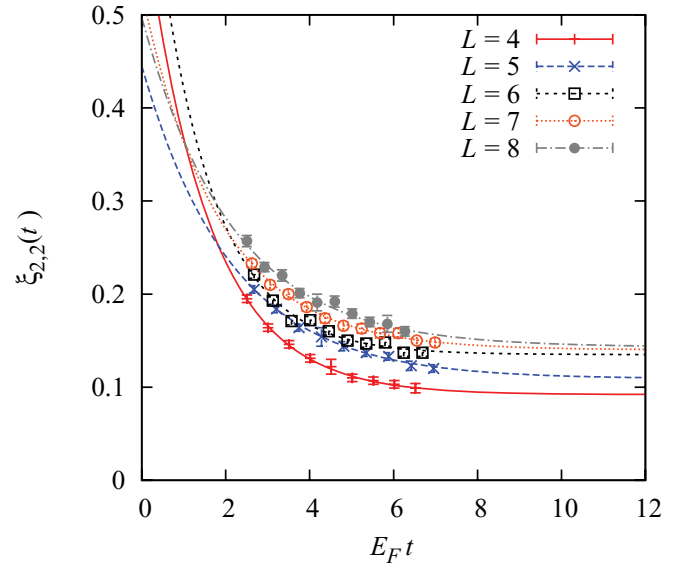|		L^3		
4^3	5^3	6^3	7^3	8^3
30	50	72	96	120
36	60	84	112	140
L_t ⋮	⋮	⋮	⋮	⋮
78	130	180	256	300

FIG. 4. (Color online) The lattice data for $\xi_{2,2}(t)$ versus $E_F t$ for $L = 4,5,6,7,8$. Also shown are the results of the asymptotic fits.

in Ref. [51,52,62,63]. We focus on measuring the ground-state energy accurately and ignore the numerically small contributions hidden in the far asymptotic tail of $\xi_{2,2}(t)$. We determine b, δE, and $\xi_{2,2}$ from least-squares fitting over the range $E_F t = 2$ to $E_F t = 6$. The lattice data for $\xi_{2,2}(t)$ together with the asymptotic fits are shown in Fig. 4.

We use the lattice results for $\xi_{2,2}$ with $L = 4,5,6,7,8$ to extrapolate to the continuum limit $L \to \infty$. In Fig. 5 we show the lattice results for $\xi_{2,2}$ for $L = 4,5,6,7,8$ plotted versus L^{-1}. We expect a dependence on L arising from effects such as the effective range correction and lattice cutoff effects. Using a
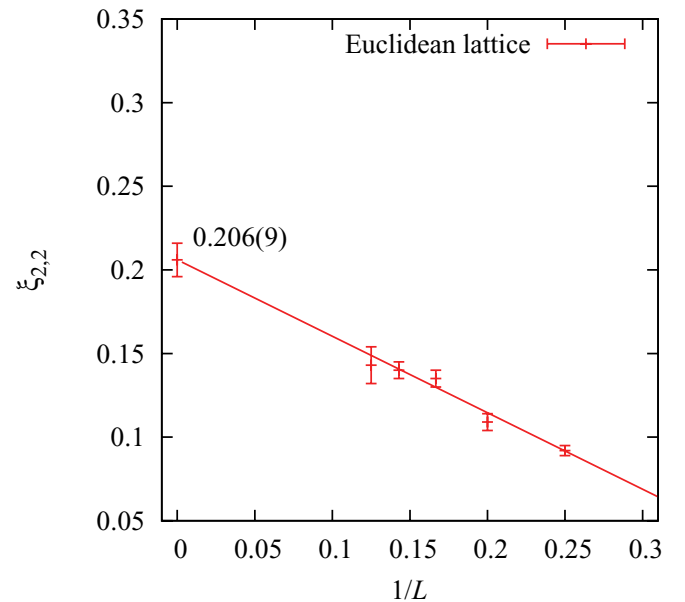

FIG. 5. (Color online) Results for $\xi_{2,2}$ for $L = 4,5,6,7,8$ plotted versus L^{-1}. The lattice results are extrapolated to the continuum limit $L \to \infty$.

linear extrapolation in L^{-1}, we obtain the continuum limit value

$$\xi_{2,2} = 0.206(9). \tag{36}$$

This result using the Euclidean lattice projection Monte Carlo method is in agreement with the Hamiltonian lattice results in Eqs. (19) and (20).

VI. DIFFUSION MONTE CARLO METHODS WITH FIXED AND RELEASED NODES

A. Formalism and notation

We now discuss diffusion Monte Carlo calculations for the same benchmark system of four particles at unitarity in a periodic cube with length L. This time, however, we use continuous variables and consider the evolution as a function of Euclidean time as a diffusion Monte Carlo process using an ensemble of random walkers. An introduction to the basic techniques can be found in Ref. [69]. For the interaction between spin-up and spin-down fermions we use a Pöschl-Teller potential tuned to infinite S-wave scattering length. For fermion mass m, the form of the potential is

$$V(r) = -\frac{2}{m}\frac{\mu^2}{\cosh^2(\mu r)}, \tag{37}$$

where the momentum scale μ determines the S-wave effective range parameter,

$$r_0 = 2\mu^{-1}. \tag{38}$$

The unitarity limit corresponds with taking the limit $\mu \to \infty$. For the unpolarized four-particle system we let $\mathbf{R}$ be the set of individual particle coordinates,

$$\mathbf{R} = \{\vec{r}_{1_\uparrow}, \vec{r}_{1_\downarrow}, \vec{r}_{2_\uparrow}, \vec{r}_{2_\downarrow}\}. \tag{39}$$

We use a BCS-type pairing wave function projected onto two spin-up and two spin-down fermions. The wave function $\Psi_{\mathrm{BCS}}(\mathbf{R})$ can be written as a 2×2 Slater determinant,

$$\Psi_{\mathrm{BCS}}(\mathbf{R}) = \det\begin{bmatrix} \phi(\vec{r}_{1_\uparrow} - \vec{r}_{1_\downarrow}) & \phi(\vec{r}_{1_\uparrow} - \vec{r}_{2_\downarrow}) \\ \phi(\vec{r}_{2_\uparrow} - \vec{r}_{1_\downarrow}) & \phi(\vec{r}_{2_\uparrow} - \vec{r}_{2_\downarrow}) \end{bmatrix}, \tag{40}$$

where $\phi(\vec{r})$ is the pairing function. The trial wave function $\Psi_T(\mathbf{R})$ is given as a product of $\Psi_{\mathrm{BCS}}(\mathbf{R})$ times a Jastrow factor [70],

$$\Psi_T(\mathbf{R}) = \Psi_{\mathrm{BCS}}(\mathbf{R})\exp[J(\mathbf{R})]. \tag{41}$$

The Jastrow factor incorporates particle correlations and is useful in reducing stochastic errors in the Monte Carlo calculation [71–74]. We use a product of Gaussian functions for the Jastrow factor. The exponents of these Gaussian functions are tuned to minimize the combination of the variational energy and the variance of the local energy in the variational Monte Carlo method. We note that the positive definite function $\exp[J(\mathbf{R})]$ has no effect on the nodal structure of $\Psi_T(\mathbf{R})$.

To determine the pairing function $\phi(\vec{r})$ we use an approach similar to that in Ref. [36]. We use an ansatz that is a superposition of Gaussian functions with periodic copies,

$$\phi(\vec{r}) = \sum_k d_k \sum_{s_x,s_y,s_z=-1}^{1} e^{-\frac{\alpha_k}{2}(x+s_x L)^2} e^{-\frac{\alpha_k}{2}(y+s_y L)^2} e^{-\frac{\alpha_k}{2}(z+s_z L)^2}. \tag{42}$$

Here $\vec{r} = (x,y,z)$, and d_k and α_k are variational parameters. Gaussian functions from the nearest periodic images at distance L make small contributions, while periodic copies farther away can be neglected. This construction has the advantage of providing more flexibility for pairing orbitals in the box while keeping the orbitals smooth over the periodic boundary with zero derivative. The Jastrow factor $\exp[J(\mathbf{R})]$ is constructed similarly. The calculation is performed using standard variational Monte Carlo sampling of the square of the trial function [69,75].

For the diffusion Monte Carlo calculation we use a large ensemble of forward-propagating random walkers with population branching processes determined by the local energy and guided by the trial wave function $\Psi_T(\mathbf{R})$. The local density of random walkers gives a statistical estimate of the product of the propagated quantum wave function $\Psi(\mathbf{R})$ times the $\Psi_T(\mathbf{R})$ trial function. In the fixed-node (FN) diffusion Monte Carlo (DMC) calculation, the nodal structure of $\Psi(\mathbf{R})$ is fixed by $\Psi_T(\mathbf{R})$, and the product $\Psi(\mathbf{R})\Psi_T(\mathbf{R})$ is therefore positive definite. Since the trial function is known explicitly and analytically, it is then possible to extract the energetics of the lowest fermionic state within the fixed-node boundary conditions [69,75].

The fixed-node calculation sets an upper bound on the ground-state energy. To measure the quality of the upper bound we release the nodal constraints [76]. For the released-node (RN) DMC calculation we use a positive-definite guiding profile for the diffusion of random walkers. In the calculations presented here we consider a one-parameter family of guiding profiles,

$$\Psi_G^\alpha(\mathbf{R}) = \sqrt{\Psi_T^2(\mathbf{R}) + \alpha\langle\Psi_T^2\rangle}. \tag{43}$$

The dimensionless parameter α controls the rate of diffusion across the nodal boundaries of $\Psi_T(\mathbf{R})$, and $\langle\Psi_T^2\rangle$ is the average value of $\Psi_T^2(\mathbf{R_0})$ evaluated over all $\mathbf{R_0}$, where $\mathbf{R_0}$ is the configuration right after the nodal release process.

B. Results for the four-particle benchmark

In Fig. 6 we show fixed-node (FNDMC) and released-node (RNDMC) diffusion Monte Carlo results for two spin-up and spin-down fermions in a periodic cube at unitarity. The ratio of the effective range parameter to the length of the cube is $r_0/L = 1/40$. We use parameters $\alpha = 0.01, 0.05, 0.2$ for the guiding profile $\Psi_G^\alpha(\mathbf{R})$. With each nodal crossing the associated weights of the random walkers change sign, leading to a sign cancellation problem that grows exponentially with Euclidean propagation time t. For the calculations presented here we have measured the released-node correction starting from the fixed-node result up to propagation time of $t = 0.4E_F^{-1}$. As
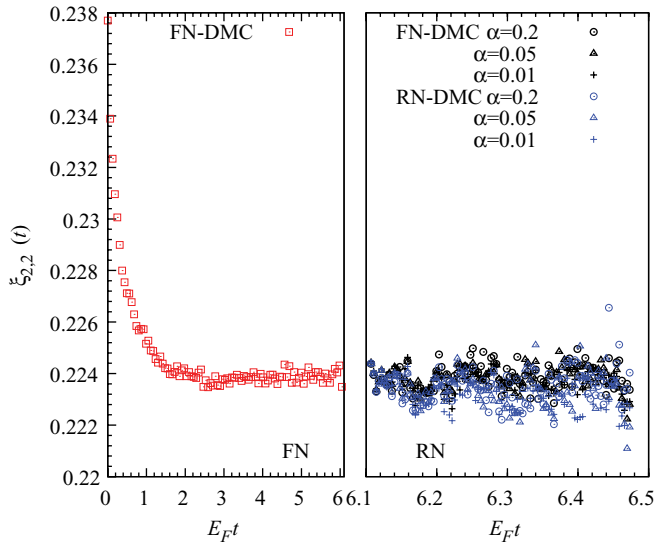
FIG. 6. (Color online) Fixed-node and released-node diffusion Monte Carlo results for $r_0/L = 0.025$ and $\alpha = 0.01, 0.05, 0.2$.

seen in Fig. 6, the decrease in $\xi_{2,2}$ is less than 0.002 over the duration of the released-node time propagation.

We have repeated the fixed-node and released-node calculations of $\xi_{2,2}$ for values of $r_0/L = 1/20, 1/40, 1/80, 1/160, 1/320, 1/640$. The fixed-node results for $\xi_{2,2}$ versus the r_0/L are shown in Fig. 7. Using a linear fit in r_0/L, we extrapolated to the limit of zero effective range.

In the zero-range limit we get the final result

$$\xi_{2,2} = 0.212(2) \qquad (44)$$

in the fixed-node approximation. The error estimate includes the stochastic error, zero-range extrapolation error, and errors due to time-step discretization and other small residual effects.
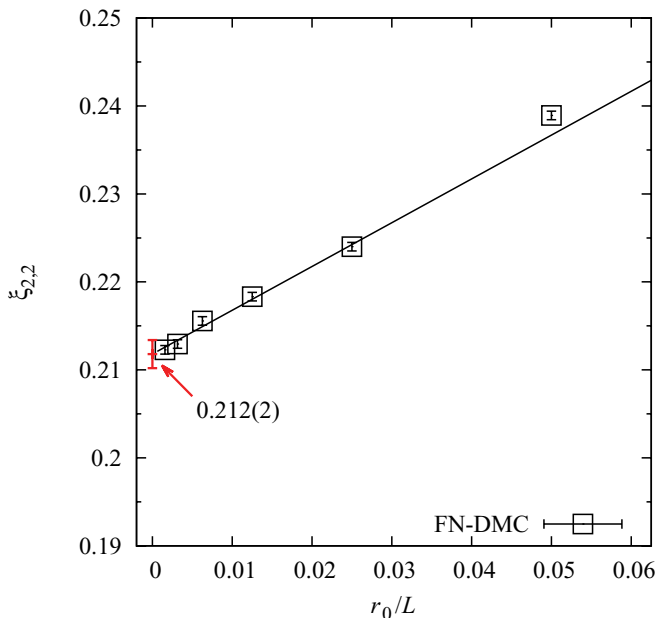

FIG. 7. (Color online) Fixed-node diffusion Monte Carlo results for $\xi_{2,2}$ versus r_0/L. The data are extrapolated to the limit of zero effective range.

The released-node calculations are quantitatively similar to the results shown in Fig. 6 for $r_0/L = 1/40$. The decrease in $\xi_{2,2}$ is less than 0.002 over a propagation time of $0.4E_F^{-1}$. We note that E_F^{-1} is the characteristic time scale required for two neighboring particles of the same spin to cross paths. Given the stochastic noise in the released-node calculation results, it is difficult to pin down a correction to the fixed-node result from the nodal release. However, a reasonable conservative estimate is that the upper bound set by the fixed-node calculation is less than $0.002/0.4 = 0.005$ above the actual value. This appears to be confirmed by the agreement of Eq. (44) with the values for $\xi_{2,2}$ obtained using the Hamiltonian lattice eigenvector iteration and the Euclidean lattice Monte Carlo method.

VII. SUMMARY AND DISCUSSION

We have presented benchmark calculations for four unpolarized particles in a periodic cube using three different methods. In the Hamiltonian lattice formalism with iterated eigenvector methods, we obtained

$$\xi_{2,2} = 0.211(2) \qquad (45)$$

using the Hamiltonian H_1 defined in Eq. (11) and

$$\xi_{2,2} = 0.210(2) \qquad (46)$$

using the Hamiltonian H_2 defined in Eq. (12). Using the Euclidean lattice formalism with the auxiliary-field projection Monte Carlo method, we found the result

$$\xi_{2,2} = 0.206(9). \qquad (47)$$

With the fixed-node diffusion Monte Carlo method in the continuum we extracted the upper bound

$$\xi_{2,2} \leqslant 0.212(2). \qquad (48)$$

The release-node Monte Carlo calculation shows a decrease in $\xi_{2,2}$ that is less than 0.002 over a propagation time of $0.4E_F^{-1}$. We estimate that the upper bound set by the fixed-node calculation is less than 0.005 above the actual value. All three methods agree within estimated errors. The unpolarized four-particle benchmarks presented here should be useful for testing and calibrating residual errors for other numerical methods and perhaps also analytical calculations. We note that the comparison requires using the few-body definition of $\xi_{2,2}$ in Eq. (3). If the thermodynamical definition in Eq. (7) is used, then the conversion factor is $\xi_{2,2} = 0.7331\xi_{2,2}^{\text{thermo}}$.

We note the importance of continuum limit extrapolations for lattice calculations and zero-range limit extrapolations for continuum diffusion Monte Carlo calculations. The importance of continuum limit extrapolations in lattice calculations was already noted and measured in Ref. [52]. In the fixed-node diffusion Monte Carlo calculations presented here we find that r_0/L needs to be less than 0.03 in order to obtain a value for $\xi_{2,2}$ that is accurate to a relative error of 0.1. This is consistent with the range dependence found in Ref. [42]. After discussion with the authors of Ref. [42], we were informed that they obtained an upper bound for $\xi_{2,2}$ from the fixed-node diffusion Monte Carlo method that agrees within two significant digits with the results reported here.

In this paper the four-particle benchmark was chosen to allow comparisons among several very different numerical methods. For larger $N = N_\uparrow = N_\downarrow$ systems it is unfortunately not possible to use iterated eigenvector methods due to exponential L^{6N-3} scaling in memory. However, the Euclidean lattice Monte Carlo and diffusion Monte Carlo methods extend readily to larger systems, and it is useful to comment on the relationship between the four-particle calculations discussed here and calculations in larger systems at unitarity.

The four-particle results presented here should be useful for comparisons of different lattice Monte Carlo calculations using different lattice actions and algorithms. We note that there is a significant correction produced by the extrapolation to the continuum limit. For some lattice actions this extrapolation decreases the ground-state energy, while for others it increases the ground-state energy. In all cases it is important that stochastic and systematic errors are sufficiently small for each chosen lattice spacing so that the continuum extrapolation can be done accurately. The same lattice methods used here to find $\xi_{2,2} = 0.206(9)$ were also used to determine $\xi_{5,5} = 0.292(12)$ and $\xi_{7,7} = 0.329(5)$ in Ref. [52]. In order to benchmark different lattice Monte Carlo methods, one starting point would be to test agreement with each of these values for $\xi_{N,N}$.

The fixed-node diffusion Monte Carlo methods presented here were also applied to larger $N = N_\uparrow = N_\downarrow$ systems at unitarity. In Ref. [77] the results $\xi_{7,7} \leqslant 0.407(2)$, $\xi_{19,19} \leqslant 0.409(3)$, and $\xi_{33,33} \leqslant 0.398(3)$ are presented. These results are comparable to the upper bounds found in Ref. [42], and in each case a significant reduction in the ground-state energy is seen when extrapolating to the zero-range limit. For the released-node calculations in these larger systems, the exponential severity of sign cancellations makes it difficult to extract data for Euclidean propagation time t greater than $N^{-1}E_F^{-1}$. As noted above, E_F^{-1} is the characteristic time scale required for two neighboring particles of the same spin to cross paths. For $N = 2$ we extrapolated to get a bound on the decrease in $\xi_{2,2}$ over a propagation time of E_F^{-1}. For larger N the extrapolation from propagation time $N^{-1}E_F^{-1}$ to time E_F^{-1}

cannot be done reliably, and this is seen already for the case $N = 7$ [77].

We note that there remains a significant gap between the lattice result $\xi_{7,7} = 0.329(5)$ and the fixed-node upper bound $\xi_{7,7} \leqslant 0.407(2)$. This discrepancy must be better understood. A good starting point would be to make benchmark comparisons for other small systems, $N = 3,4,5$. First, it should be established that different lattice calculations agree on the values for $\xi_{3,3}$, $\xi_{4,4}$, and $\xi_{5,5}$. Next, the difference between lattice and fixed-node results should be measured for each N. The key question then is if this difference can be resolved by released-node calculations for smaller values of N. Given the agreement for $\xi_{2,2}$, there is some reason to suggest that this may be possible.

---

[1] D. M. Eagles, Phys. Rev. **186**, 456 (1969).

[2] A. J. Leggett, in *Modern Trends in the Theory of Condensed Matter. Proceedings of the XVIth Karpacz Winter School of Theoretical Physics, Karpacz, Poland, 1980* (Springer, Berlin, 1980), p. 13.

[3] P. Nozieres and S. Schmitt-Rink, J. Low Temp. Phys. **59**, 195 (1985).

[4] K. M. O'Hara, S. L. Hemmer, M. E. Gehm, S. R. Granade, and J. E. Thomas, Science **298**, 2179 (2002).

[5] S. Gupta, Z. Hadzibabic, M. W. Zwierlein, C. A. Stan, K. Dieckmann, C. H. Schunck, E. G. M. van Kempen, B. J. Verhaar, and W. Ketterle, Science **300**, 1723 (2003).

[6] C. A. Regal and D. S. Jin, Phys. Rev. Lett. **90**, 230404 (2003).

[7] T. Bourdel, J. Cubizolles, L. Khaykovich, K. M. F. Magalhaes, S. J. J. M. F. Kokkelmans, G. V. Shlyapnikov, and C. Salomon, Phys. Rev. Lett. **91**, 020402 (2003).

[8] M. E. Gehm, S. L. Hemmer, S. R. Granade, K. M. O'Hara, and J. E. Thomas, Phys. Rev. A **68**, 011401(R) (2003).

[9] M. Bartenstein, A. Altmeyer, S. Riedl, S. Jochim, C. Chin, J. H. Denschlag, and R. Grimm, Phys. Rev. Lett. **92**, 120401 (2004).

[10] T. Bourdel, L. Khaykovich, J. Cubizolles, J. Zhang, F. Chevy, M. Teichmann, L. Tarruell, S. J. J. M. F. Kokkelmans, and C. Salomon, Phys. Rev. Lett. **93**, 050401 (2004).

[11] J. Kinast, A. Turlapov, J. E. Thomas, Q. Chen, J. Stajic, and K. Levin, Science **307**, 1296 (2005).

[12] G. B. Partridge, W. Li, R. I. Kamar, Y. Liao, and R. G. Hulet, Science **311**, 503 (2006).

[13] J. T. Stewart, J. P. Gaebler, C. A. Regal, and D. S. Jin, Phys. Rev. Lett. **97**, 220406 (2006).

[14] J. Joseph, B. Clancy, L. Luo, J. Kinast, A. Turlapov, and J. E. Thomas, Phys. Rev. Lett. **98**, 170401 (2007).

[15] L. Tarruell, M. Teichmann, J. Mckeever, T. Bourdel, J. Cubizolles, L. Khaykovich, J. Zhang, N. Navon, F. Chevy, and C. Salomon, in *Ultra-Cold Fermi Gases*, Proceedings of the International School of Physics "Enrico Fermi," Course CLXIV (IOS Press, Amsterdam, 2008).

[16] L. Luo and J. E. Thomas, J. Low Temp. Phys. **154**, 1 (2009).
[17] M. Zwierlein (unpublished).
[18] J. R. Engelbrecht, M. Randeria, and C. A. R. Sa de Melo, Phys. Rev. B **55**, 15153 (1997).
[19] R. Haussmann, W. Rantner, S. Cerrito, and W. Zwerger, Phys. Rev. A **75**, 023610 (2007).
[20] G. A. Baker, Phys. Rev. C **60**, 054311 (1999).
[21] H. Heiselberg, Phys. Rev. A **63**, 043606 (2001).
[22] H. Hu, P. D. Drummond, and X. Liu, Nat. Phys. **3**, 469 (2007).
[23] A. Perali, P. Pieri, and G. C. Strinati, Phys. Rev. Lett. **93**, 100404 (2004).
[24] H. S. Köhler (2010), e-print arXiv:1008.3884.
[25] T. Papenbrock, Phys. Rev. A **72**, 041603(R) (2005).
[26] B. Krippa, J. Phys. A **42**, 465002 (2009).
[27] J. V. Steele (2000), e-print arXiv:nucl-th/0010066.
[28] T. Schäfer, C.-W. Kao, and S. R. Cotanch, Nucl. Phys. A **762**, 82 (2005).
[29] Y. Nishida and D. T. Son, Phys. Rev. Lett. **97**, 050403 (2006).
[30] Y. Nishida and D. T. Son, Phys. Rev. A **75**, 063617 (2007).
[31] J.-W. Chen and E. Nakano, Phys. Rev. A **75**, 043620 (2007).
[32] P. Arnold, J. E. Drut, and D. T. Son, Phys. Rev. A **75**, 043605 (2007).
[33] Y. Nishida, Phys. Rev. A **79**, 013627 (2009).
[34] P. Nikolic and S. Sachdev, Phys. Rev. A **75**, 033608 (2007).
[35] J. Chen, Chin. Phys. Lett. **24**, 1825 (2007).
[36] J. Carlson, S. Y. Chang, V. R. Pandharipande, and K. E. Schmidt, Phys. Rev. Lett. **91**, 50401 (2003).
[37] G. E. Astrakharchik, J. Boronat, J. Casulleras, and S. Giorgini, Phys. Rev. Lett. **93**, 200404 (2004).
[38] J. Carlson and S. Reddy, Phys. Rev. Lett. **95**, 060401 (2005).
[39] V. K. Akkineni, D. M. Ceperley, and N. Trivedi, Phys. Rev. B **76**, 165116 (2007).
[40] O. Juillet, New J. Phys. **9**, 163 (2007).
[41] A. J. Morris, P. López Ríos, and R. J. Needs, Phys. Rev. A **81**, 033619 (2010).
[42] M. McNeil Forbes, S. Gandolfi, and A. Gezerlis (2010), e-print arXiv:1011.2197.
[43] D. Lee and T. Schäfer, Phys. Rev. C **73**, 015201 (2006).
[44] D. Lee and T. Schäfer, Phys. Rev. C **73**, 015202 (2006).
[45] A. Bulgac, J. E. Drut, and P. Magierski, Phys. Rev. Lett. **96**, 090404 (2006).
[46] E. Burovski, N. Prokofev, B. Svistunov, and M. Troyer, Phys. Rev. Lett. **96**, 160402 (2006).
[47] E. Burovski, N. Prokofev, B. Svistunov, and M. Troyer, New J. Phys. **8**, 153 (2006).
[48] T. Abe and R. Seki, Phys. Rev. C **79**, 054002 (2009).
[49] T. Abe and R. Seki, Phys. Rev. C **79**, 054003 (2009).
[50] A. Bulgac, J. E. Drut, and P. Magierski, Phys. Rev. A **78**, 023625 (2008).
[51] D. Lee, Phys. Rev. B **73**, 115112 (2006).
[52] D. Lee, Phys. Rev. C **78**, 024001 (2008).
[53] D. Lee, Eur. Phys. J. A **35**, 171 (2008).
[54] J.-W. Lee, M. G. Endres, D. B. Kaplan, and A. N. Nicholson, e-print arXiv:1011.3026.
[55] M. G. Endres, D. B. Kaplan, J.-W. Lee, and A. N. Nicholson, e-print arXiv:1011.3089.
[56] M. Lüscher, Commun. Math. Phys. **105**, 153 (1986).
[57] S. R. Beane, P. F. Bedaque, A. Parreno, and M. J. Savage, Phys. Lett. B **585**, 106 (2004).
[58] R. Seki and U. van Kolck, Phys. Rev. C **73**, 044006 (2006).
[59] B. Borasoy, E. Epelbaum, H. Krebs, D. Lee, and U.-G. Meißner, Eur. Phys. J. A **31**, 105 (2007).
[60] C. Lanczos, J. Res. Natl. Bur. Stand. (U S) **45**, 255 (1950).
[61] D. Lee and R. Thomson, Phys. Rev. C **75**, 064003 (2007).
[62] D. Lee, Phys. Rev. B **75**, 134502 (2007).
[63] D. Lee, Prog. Part. Nucl. Phys. **63**, 117 (2009).
[64] M. Creutz, Phys. Rev. D **38**, 1228 (1988).
[65] M. Creutz, Found. Phys. **30**, 487 (2000).
[66] R. T. Scalettar, D. J. Scalapino, and R. L. Sugar, Phys. Rev. B **34**, 7911 (1986).
[67] S. Gottlieb, W. Liu, D. Toussaint, R. L. Renken, and R. L. Sugar, Phys. Rev. D **35**, 2531 (1987).
[68] S. Duane, A. D. Kennedy, B. J. Pendleton, and D. Roweth, Phys. Lett. B **195**, 216 (1987).
[69] W. Foulkes, L. Mitas, R. Needs, and G. Rajagopal, Rev. Mod. Phys. **73**, 33 (2001).
[70] R. Jastrow, Phys. Rev. **98**, 1479 (1955).
[71] C. J. Umrigar, K. G. Wilson, and J. W. Wilkins, Phys. Rev. Lett. **60**, 1719 (1988).
[72] K. E. Schmidt and J. W. Moskowitz, J. Chem. Phys. **93**, 4172 (1990).
[73] L. Mitas and R. M. Martin, Phys. Rev. Lett. **72**, 2438 (1994).
[74] J. C. Grossman, L. Mitas, and K. Raghavachari, Phys. Rev. Lett. **75**, 3870 (1995).
[75] M. Bajdich and L. Mitas, Acta Phys. Slovaca **59**, 81 (2009).
[76] D. Ceperley and B. Alder, J. Chem. Phys. **81**, 12 (1984).
[77] X. Li, J. Kolorenc, and L. Mitas (2011), e-print arXiv:1105.1748v2.